Nuclear Instruments and Methods in Physics Research A 768 (2014) 112–119

Contents lists available at ScienceDirect

Nuclear Instruments and Methods in Physics Research A

journal homepage: www.elsevier.com/locate/nima

Intensity control in experimental rooms of the GANIL accelerator

C. Courtois *, C. Jamet, W. Le Coz, G. Ledu

GANIL, CEA/DSM - CNRS/IN2P3, Bd Henri Becquerel, BP 55027, F-14076 Caen Cedex 5, France

ARTICLE INFO

Article history:
Received 9 July 2014
Received in revised form
22 August 2014
Accepted 15 September 2014
Available online 22 September 2014

Keywords:
Beam current monitors
Particle beam diagnostics
Fast toroids
Capacitive pick-up
Cyclotron

ABSTRACT

The safety re-examination of existing GANIL (the French national heavy-ion accelerator facility) installations requires the implementation of a safety system which makes possible the monitoring of beam intensities sent in the experimental rooms. The aim is to demonstrate that beam intensities stay below the authorized limits. The required characteristics should enable the measurement, by a non-interceptive method, of beam intensities from 5 nA to 5 μA with a maximum uncertainty of ±5%, independently of the frequency and the beam energy. After a comparative study, two high frequency diagnostics were selected: the capacitive Pick-Up (PU) and the Fast Current Transformer (FCT). Based on results of simulation, laboratory tests and machine studies, this paper discusses all the considerations required to deliver accurate results from PU and FCT measurement of ion beams.

1. Introduction

GANIL (the French national heavy-ion accelerator facility) is an economic interest group managed jointly by the Physical Science Division (DSM) of the French Atomic Energy Commission (CEA) and the National Institute of Nuclear and Particle Physics (IN2P3) of the National Center for Scientific Research (CNRS). Its vocation is to provide to the scientific community the means to carry out experiments in atomic and nuclear physics. The facility produces, thanks to several cyclotrons running in cascade, a wide spectrum of high intensity ion beams ranging from ^{12}C to ^{238}U accelerated up to 96 MeV/u [1,2]. For stable beam production and acceleration, two large separated sectors' cyclotrons (CSS1 and CSS2) are used after the injector cyclotron. Additionally, radioactive beams can be delivered by the cyclotron CIME (SPIRAL post-accelerator). As a basic nuclear facility, GANIL is subject to the obligations laid down in the decree of February 7, 2012. Following the issuance of this order, a safety review of GANIL has been required by the Nuclear Safety Authorities (ASN).

In the context of this safety re-examination, the beam intensity monitoring has to be upgraded to protect personnel from radiation hazards. Until now, AC Current Transformers (ACCT) have measured the beam transmission through the beam lines and the cyclotrons [3]. To use this kind of diagnostic, the beam must be interrupted by a chopper at a low frequency (hundred of Hz). Correct operation of this system depends on the synchronization of ACCTs and chopper which is highly complicated by the variable time of flight of GANIL and the different locations of the diagnostics along the beam line. These devices do not provide the level of safety required.

A system, that controls the beam intensity delivered in experimental rooms in the energy (1.7–96 MeV/u) and frequency (7–14.5 MHz) ranges used at GANIL, is thus expected to be developed. At the end of the project, several equipments will be installed in beam lines and experimental rooms. All of them will be classified as Element Important to Protection (EIP). They have thus to meet a number of requirements in terms of safety, in particular, that correct operation is as strongly ensured as possible.

2. Requirements

The system has to demonstrate that the maximal beam intensities sent in experimental rooms, as defined in the general operating rules of GANIL, are respected. A second objective is to detect beam losses. Instruments for monitoring the beam intensity must not impose any form of physical obstruction on the beam trajectory and should be independent of beam position, temperature, frequency, energy and phase extension. The system has to provide a highly reliable measure of the mean beam intensity with a relative precision better than ±5% in the range of 5 nA to 5 μA.

2.1. Quality assurance/quality control process

In addition to general specifications, a QA/QC Process has to be followed. During the planning and the development, some activities have to be performed to establish the reliability of the product, such

* Corresponding author. Tel.: +33 2 31 45 47 09.
E-mail address: courtois@ganil.fr (C. Courtois).

http://dx.doi.org/10.1016/j.nima.2014.09.044
0168-9002/

as the characterization of the measurement chain in laboratory. The use of approved standardized procedures for emission and removal calculations, measurements and estimating uncertainties is required.

One of the fundamental safety requirements is to check that the beam intensity limit is not exceeded. In order to avoid exceeding the limit, the threshold has to take into account the global measurement uncertainty. Thus the uncertainty has to be as low as possible. The uncertainty has to be characterized as its influence quantities:

- beam energy,
- beam phase extension,
- beam lateral position,
- temperature,
- frequency,
- external magnetic fields.

All these influence quantities generate systematic errors which have to be taken into account. Dispersion measurements are discussed in this paper.

3. Technical solutions

Instruments for monitoring the beam intensity in a circular accelerator must not impose any form of physical obstruction on the beam trajectory and should be independent of beam position. Capacitive Pick-Ups (PU) and all current transformers meet these demands [4]. However, as explained in the introduction, AC current transformers have been abandoned in favor of Fast Current Transformers (FCT). FCTs allow viewing the temporal structure of the beam current and cover the entire GANIL frequency range. The PU and the FCT have thus been selected. The principle of the PU is the detection of the electric field carried by the beam, while the FCT detects the accompanied magnetic field.

The energy sensitivity of the electrical field generated by a charged particle has been widely studied and demonstrated, while the energy sensitivity of the magnetic field is not really described in the scientific literature. These two diagnostics have been confronted in machine studies.

3.1. FCT features

The toroidal FCT, type FCT-ISOF8-96.0-40-UHV-05:1, was manufactured by Bergoz Instrumentation (Fig. 1) [5]. The main feature of the FCT is its large bandwidth (up to 2 GHz). This bandwidth allows the FCT to restitute the high frequency variations of the beam signal. The number of turns has been optimized to give a sensibility of 5 V/A. Connected to an amplifier with 50 Ω impedance, the transformer yields nominal signal amplitude of:

$$\begin{aligned} V_{\text{signal}} &= \frac{I_{beam}}{5\ \text{turns}} \times \left(\frac{1}{50\ \Omega}+\frac{1}{50\ \Omega}\right)^{-1} \\ &= 5\ \text{V/A} \times I_{\text{beam}} \\ &= 50\ \Omega \times \tau_{\text{FCT}} \times I_{\text{beam}} \end{aligned} \quad (1)$$

with the FCT transmittance $\tau_{\text{FCT}} = 1/10$ and the beam current I_{beam}. This equation is sketched in the article of Nantista and Adolphsen [6].

3.2. PU features

The PU is a cylindrical electrode designed and manufactured by GANIL. The capacitance formed by the surface of the electrode and the grounded wall is around 37 pF. This value results from a compromise between a low thermal noise get with a strong capacity and a strong output signal obtained with a low capacity. To preserve the charge distribution, the load impedance seen by the electrode is a high impedance.

4. Signal processing

The minimal intensity which has to be measured is 5 nA. With a sensibility of 5 V/A, a 5 nA beam corresponds to a signal of 25 nV out of the diagnostic. This level is really low compared to a required 5% total accuracy in the accelerator environment where electromagnetic disturbances are extreme. Signal processing needs thus many considerations.

4.1. FCT signal processing

As sketched in Fig. 2, the FCT does not transform DC components. The direct measurement of the mean current h_0 is thus not permitted.

The DC component can be calculated from other harmonic components by assuming electromagnetic field lines seen by FCT and PU fall to zero between pulses. Many harmonics are created since the beams from cyclotrons are a chain of short pulses with a constant repetition rate.

The noise observed without beam crossing the diagnostics has components induced by the RF system. As the fundamental is disturbed by the RF power amplifiers, higher harmonic components are examined. Since proportionality between the amplitude of the second harmonic component and beam current is quite stable, h_2 is selected. For a Gaussian distribution, the ratio h_2/h_0 is 2. Fig. 3 shows that a Gaussian fit is relevant.

By starting from this relation, a theoretical formula of the root mean square (rms) value of the second harmonic at the terminals of the FCT versus the mean value of the beam current can be found.

$$h_2 \cong 2 \times \overline{V_{\text{signal}}}$$

$$\begin{aligned} h_{2\text{rms}} &\cong \sqrt{2} \times \overline{V_{\text{signal}}} \\ &\cong \sqrt{2} \times 50\ \Omega \times \tau_{\text{FCT}} \times \overline{I_{\text{beam}}}. \end{aligned} \quad (2)$$

The amplifier gain and the cable attenuation must be added to obtain the total transmittance of the FCT measurement chain $t_{\text{FCT}} = h_{2\text{rms}}/\overline{I_{\text{beam}}}$.

4.2. PU signal processing

The PU signal processing is based on the second harmonic measurement as for FCT signal processing. A theoretical formula for the second harmonic output of the cylindrical probe can be also found by starting from the following relations:

- $\beta c \cong 10^7\sqrt{2w}$ the ions velocity with w being the beam energy (in MeV/u).

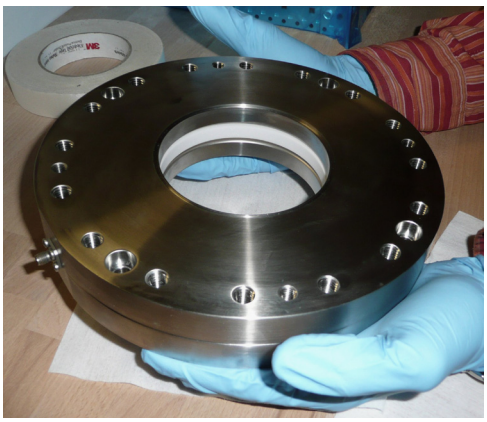

Fig. 1. FCT developed by Bergoz instrumentation.

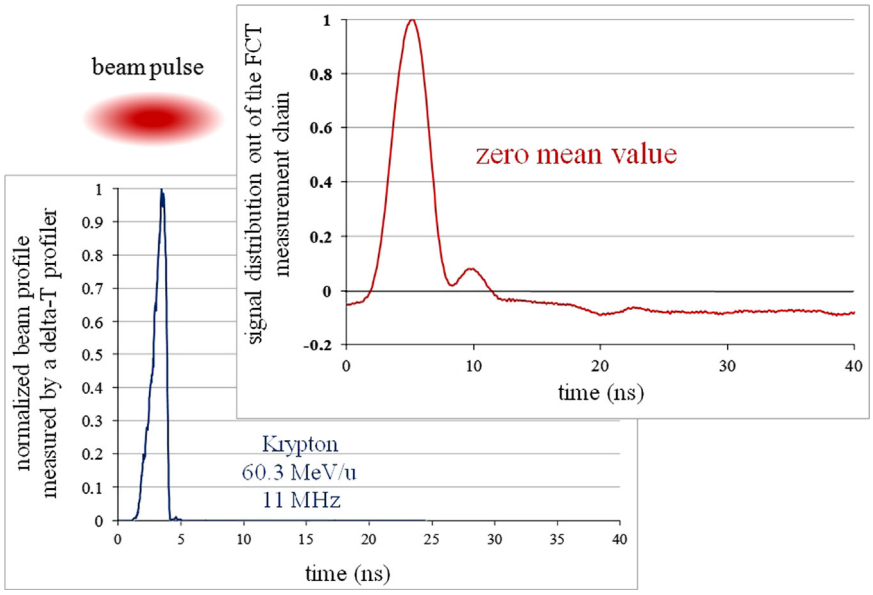

Fig. 2. Beam profile measured by a delta-T profiler and corresponding FCT signal distribution.

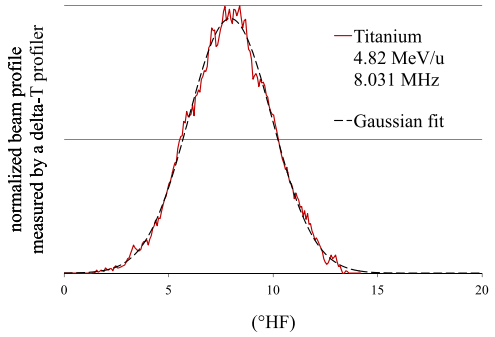

Fig. 3. Profile of a titanium beam and its Gaussian fit.

- $Q \cong L/\beta c \times \overline{I_{\text{beam}}}$ the charge deposited on the electrode supposed to be equal to the sum of all charges within the bunch Q_{bunch} with L being the electrode length of 30 mm.
- $\overline{V} \cong (Q_{bunch}/C)k(L/\beta c\Delta t)1/(1+R/L)$ the estimation for high impedance signal processing of the expected signal output of the probe [7] with C being the equivalent capacity created by the electrode when the beam is inside, Δt being the bunch length in time (FWHM) and R being the probe radius of 48 mm. For very short bunches $\beta c\Delta t \ll L$, the product of $kL/\beta c\Delta t$ has to be replaced by one. One gets $\overline{V} \cong 0.38Q_{bunch}/C$.
- and the relation between second harmonic and mean value seen in the previous subsection.

The rms value of the second harmonic at the terminals of the probe is thus given by

$$h_2 \cong 2 \times \overline{V}$$

$$\begin{aligned} h_{2\text{rms}} &\cong \sqrt{2}\frac{1}{1+R/L}\frac{Q}{C} \\ &\cong \sqrt{2}\frac{1}{1+R/L}\frac{L}{C\beta c} \times \overline{I_{\text{beam}}} \\ &\cong \frac{1}{1+R/L}\frac{L}{C10^7\sqrt{w}} \times \overline{I_{\text{beam}}}. \end{aligned} \tag{3}$$

The amplifier gain and the cable attenuation must be added to obtain the total transmittance of the PU measurement chain $t_{\text{PU}}(w) = h_{2\text{rms}}/\overline{I_{\text{beam}}}$. Sensitivity to energy must be observed in machine studies.

4.3. Signal processing difficulties

The amplitude distribution of the discrete Fourier components of a periodic pulse train signal depends on the length of the pulses. A change in the length of the pulses consequently causes a change in the amplitude of any harmonic signal component. The length of the pulses of FCT or PU output signal presents many influence quantities. Some quantities affect the relation of electromagnetic field generation and others impact bunch distribution.

The bunch distribution depends on beam tuning, distance covered by the beam and energy dispersion at the accelerator output. All these parameters affect the sigma of the bunch distribution and consequently the sigma of the signal distribution. Influence quantities like beam tuning make the sigma of the signal distribution hard to predict.

A single charged particle moving at $v = 2\pi r_e F/H$ creates an electrical field at the chamber wall with a longitudinal distribution $\sigma_{\overrightarrow{E}} = a/\gamma v\sqrt{2}$ where γ is the Lorentz factor, a is the chamber radius, r_e is the accelerator ejection radius and H is the cyclotron harmonic [9–11] (concerning the magnetic field no model exists in the literature). This relation shows the sensitivity to beam energy.

The sigma of the distribution, seen by the diagnostic, can be expressed as a quadratic sum [8]:

$$\sigma_{\text{signal}} = \sqrt{\sigma_0^2 + \sigma_{\text{path}}^2 + \sigma_{\overrightarrow{E/B}}^2} \tag{4}$$

- σ_0 is the sigma of the beam distribution at the cyclotron output. This value depends on the tuning and the energy dispersion.
- σ_{path} is the enlargement of the bunch take along the path covered. $\sigma_{\text{path}} = 180/\pi \times Hd/2r_e \times \triangle w/w_0$ with d being the distance covered and $\triangle w/w_0$ being the energy dispersion out of the cyclotron.
- $\sigma_{\overrightarrow{E/B}}$ is the enlargement due to electric or magnetic field.

According to a study with a Gaussian distribution, if the beam phase extension does not exceed 16° HF then the deviation to the relation $h_2 = 2 \times h_0$ stays below 1%. For a 23° HF beam the deviation is 2%. Other methods of measuring intensity, independent of the length of the pulses, have been examined. But synchronous detection has the advantage to make possible the extraction of even

weak signals in strong noise background. Faced with the challenge of measuring 5 nA in the noisy cyclotron environment, synchronous detection seems to be the better option.

5. Signal simulation

The least energy-dependent diagnostic should be chosen. The FCT achieves its measurement via the beam magnetic field while the PU measures the intensity via the beam electric field. Hence a study of the energy sensitivity of the electromagnetic field is conducted. There are few, if any, articles in the scientific literature about the magnetic field generated by beam while articles about beam electric field abound. Electric and magnetic fields are inextricably linked to each other since the magnetic field is induced by a time varying electric field through the displacement current. A Monte Carlo simulation of FCT and PU signals has been made by starting with the equations of classical electrodynamics [13–15]. Its primary goal is to model closely the physical interactions involved, the detectors' performance and the beam parameters. Its use is considered relevant, since it produces coherent and reliable results with a previous study conducted with beam. In Table 1, the expected variation of the second harmonic with respect to the range of energy for CSS1, CSS2 and CIME cyclotrons at GANIL is presented. For instance, the second harmonic amplitude of the FCT output signal is expected to vary by 0.007% between the extreme values of energy of CSS1 beams.

According to simulation results, the FCT is ten times less sensitive to energy variations than the PU. This result will be confronted with the experiment.

6. FCT characterization in laboratory

Tests were first performed at the Bergoz laboratory to ensure that the FCT meets its specifications. The most stringent of these is the uncertainty with temperature and frequency which has to be at most equal to 1%. Bergoz instrumentation improved the standard FCT to meet this specification.

Tests carried out at GANIL aimed at a more detailed characterization. They were conducted with a coaxial line (Fig. 4) developed at GANIL which simulates the bunch beam. The coaxial wire method is commonly employed for simulating a field configuration inside the beam pipe. The beam and the coaxial line model are different due to the presence of fields within the beam. However a short pulse in a coaxial line has a very similar electromagnetic field distribution to that of a relativistic beam [12].

6.1. Validation tests

Firstly, the analysis of the temporal response gives a rise time of 1.75 ns, a droop of 2.7% μs^{-1} and a time constant of 30 μs. The study of the frequency response, for its part, gives a lower cutoff frequency of 6.5 kHz and an upper cutoff frequency of 268 MHz. These results are consistent with the datasheet.

Then the sensitivity to beam displacement is characterized in laboratory with the coaxial line. The coaxial line is displaced from the torus center along two orthogonal axes (10 cm excursion). A typical relative uncertainty of 0.002% mm^{-1} (enlargement factor $k=3$) is observed. Sensitivity to beam lateral position is thus negligible. A radial magnetic field of 10 mT and a parallel magnetic field of 1 mT is applied. A typical relative uncertainty of 0.54% ($k=3$) is identified. External magnetic fields have little effect on the FCT. The temperature sensitivity is also characterized. The FCT is relatively stable with respect to temperature, since a typical uncertainty of 0.45% ($k=3$) is measured over the range 6–41 °C. The typical uncertainty associated to frequency is undoubtedly the dominant term, since it is 0.73% in the frequency range 14–29 MHz. This last result involves a cumulative typical uncertainty of 0.75% in the temperature and frequency ranges 6–41 °C and 14–29 MHz i.e. less than 1%.

Table 1
Simulation results.

Cyclotron – beam energy	FCT (%)	PU (%)
CSS1 up to 13.7 MeV/u	0.007	0.07
CSS2 up to 96 MeV/u	0.01	0.1
CIME 1.7–25 MeV/u	0.9	8

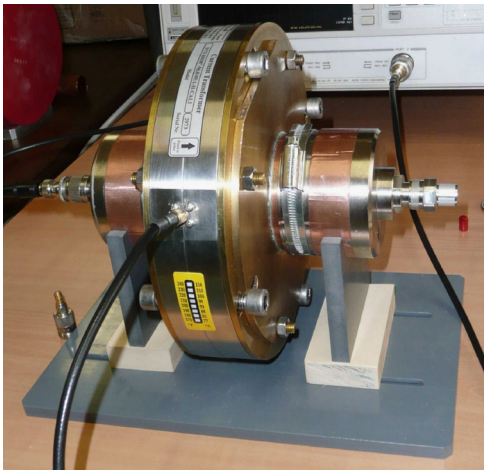

Fig. 4. Tests in laboratory with coaxial line.

6.2. Linearity in laboratory

The aim of the linearity test is to check that the relation between the delivered intensity and the measured intensity is truly linear. Figs. 5 and 6 present the performance of the FCT in terms of linearity in laboratory (with a preamplification of 49 dB). The measurement has been performed with a signal of constant frequency (20 MHz) and decreasing the intensity from 5 μA to 50 pA. The least squares method is used to find the best fit straight line. Each measuring point corresponds to the mean of one hundred measurements done with a sampling time of 0.3 s.

At 1 nA, the deviation from the regression line is 5% and rapidly falls below the percent level. Using the normal full scale, the non-linearity error of FCT does not exceed 1% FS (full scale) on [1 nA; 5 μA] and equals 6.5%FS on [50 pA; 1 nA] which is in good agreement with the desired specifications.

7. Machine studies

A prototype of each diagnostics, FCT and PU, has been set up on a beam line. Then a campaign of machine studies has been conducted with a large panel of ion beams. The aim is to cover a wide intensity range and evaluate linearity, sensitivity and resolution of diagnostics.

7.1. Measurement channels

The signal coming from the FCT is first amplified by the two low noise amplifiers of API Technologies (6719 and 6143) set close to the diagnostic. This amplification allows the transmission of the signal over 50 Ω cable to a measuring instrument, called Lock-In amplifier, outside the experimental room. The RF Lock-In Amplifier Model SR844 is manufactured by Stanford Research Systems. Its

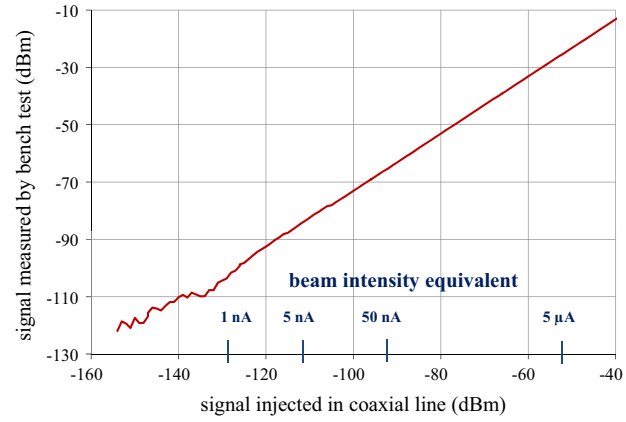

Fig. 5. Measurement chain linearity with coaxial line.

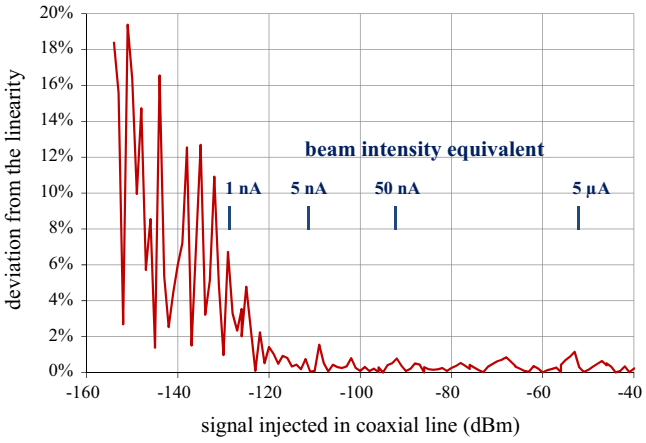

Fig. 6. Deviation from linearity with coaxial line.

frequency range of 25 kHz to 200 MHz is suitable for our purpose. Its function of interest is the harmonic detection (F and $2F$). The SR844 is adjusted for automatic detection of the $2F$ component and the fast fluctuations of the beam current are filtered by using a time constant of 1 s with 18 dB/octave roll off. An offset deduction is done with the SR844 for each sensitivity range below 300 μV_{rms}. A LabVIEW program collects data, averages and saves data to file. The PU channel is identical in order to be compared.

7.2. Reference sensors

It should be added that ACCT measurements were also performed. Many ACCT are incorporated at various locations along the beam line. With regard to this ACCT, used routinely at GANIL, an estimation of the FCT and PU transmittance can be calculated.

$$h_{2rms} = t \times \overline{I_{beam}}\ (\text{ACCT}). \tag{5}$$

According to previous subsections, this transmittance t has influence quantities such as the pulse width. The bunch length is achieved thanks to a delta-T profiler set close to FCT and PU. The delta-T measures the temporal beam profile and then the empiric standard deviation is calculated:

$$\sigma(^{\circ}\text{HF}) = 360F\sqrt{\frac{\sum c(\tau_i - \overline{\tau})}{\sum c}} \tag{6}$$

with c being the number of counts, τ being the temporal interval for which this number of counts have been counted and F being the machine frequency.

7.3. Linearity with beam

Figs. 7 and 8 present the performance in terms of linearity with a beam of $^{86}_{36}Kr^{34+}$. For determining the linearity deviation, the best fit straight line is calculated only with intensity values above 100 nA.

Concerning FCT, the deviation from linearity is 5% at 10 nA and 1% at 65 nA. The PU is less linear than the FCT since its deviation from linearity is 5% at 170 nA and 1% at 220 nA. Due to the loss of precision of the reference measurement, these results must be interpreted with caution. Below 10 nA, the ACCT does not measure the intensity correctly. For low intensity values, the reference measurement is thus estimated with the pepperpots ratios. However this method is a rough estimate since the pepperpots ratios depend on the beam emittance and their combination. The ratio of combined pepperpots does not correspond to the combination of pepperpots ratios taken separately. This inaccuracy of the reference measurements is probably the cause of the increasing non-linearity in the range of 1–10 nA observed Fig. 8. FCT and PU are probably better in terms of linearity than what has been observed.

7.4. Random error of measurement

When repeated measurements are done, a dispersion of the results is observed. The standard deviation of these results corresponds to the random error. This error comes from both the measurement chain and the beam. Fig. 9 shows standard deviation values normalized to mean values. One hundred measurements have been made with a sampling time of 0.3 s.

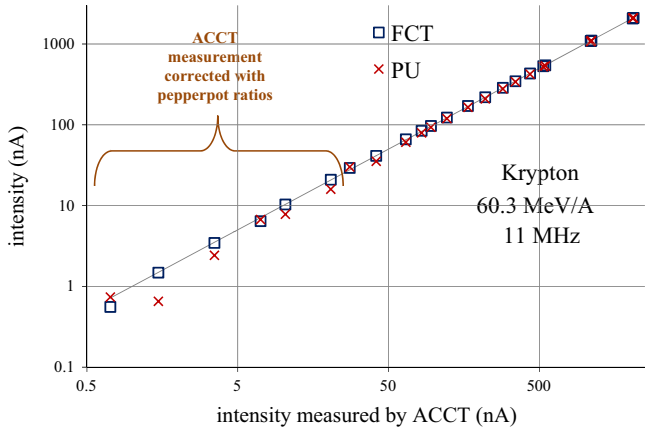

Fig. 7. Linearity with beam.

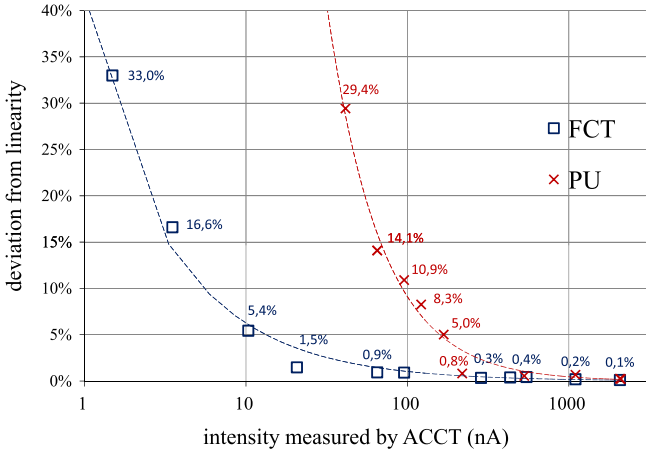

Fig. 8. Deviation from linearity.

Random errors of FCT and PU are really similar. Above 10 nA, it does not exceed the percent level for both diagnostics. It reaches 5% at 3 nA. Concerning the ACCT, the random error is more important. Indeed at 65 nA, it has been evaluated at 2%.

7.5. Sensitivity

One important purpose of beam tests is to characterize the influence of frequency, energy and pulse width on FCT and PU measurement chains. In theory, a decrease of beam energy leads to a rise of the bunch length which leads to a second harmonic level decrease.

7.5.1. FCT sensitivity

Figs. 10, 11 and 12 present the deviation from the mean of t_{FCT} versus the second harmonic frequency, the energy and the pulse width respectively. Sensitivity to frequency due to the sensor, cable and electronic instruments is assumed.

No significant dependence as a function of frequency and energy is observed. With beam sigma, it is also difficult to discern a trend. The phase extension, around four times the beam sigma, is mostly regulated by the tuning as shown in Fig. 13. These fluctuations cannot be avoided since they are due to human operation.

To conclude on the FCT sensitivity, the total uncertainty of measurement of the FCT chain is $\pm 4.9\%$ whatever the influence quantities.

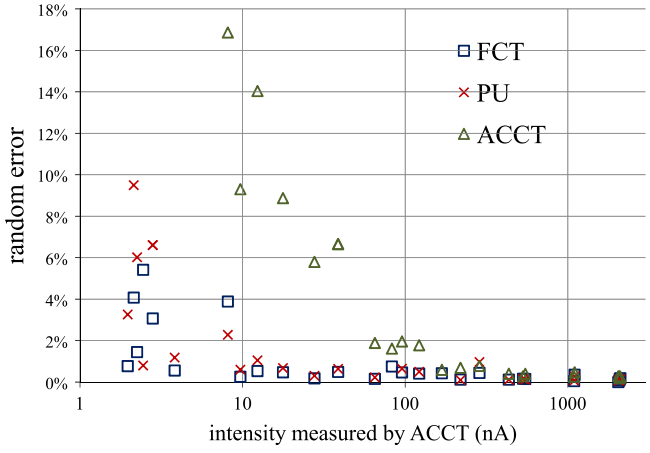

Fig. 9. Random error of measurement.

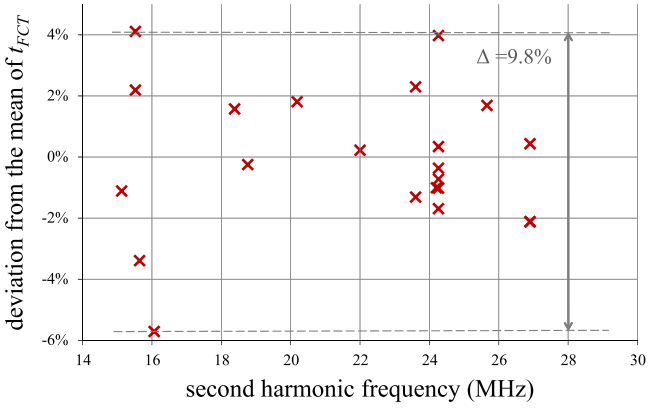

Fig. 10. Deviation from the mean of FCT transmittance versus second harmonic frequency.

7.5.2. PU sensitivity

Figs. 14 and 15 present the deviation from the mean of t_{PU} versus the second harmonic frequency and the energy respectively. Sensitivity to frequency due to the sensor, cable and electronic instruments is also assumed.

The dependence on the square root of energy can be seen. Energy varies with the square of the frequency. Frequency sensitivity is thus also observed. Once this dependency is taken into account, no further frequency sensitivity remains as shown in Fig. 16. The delta

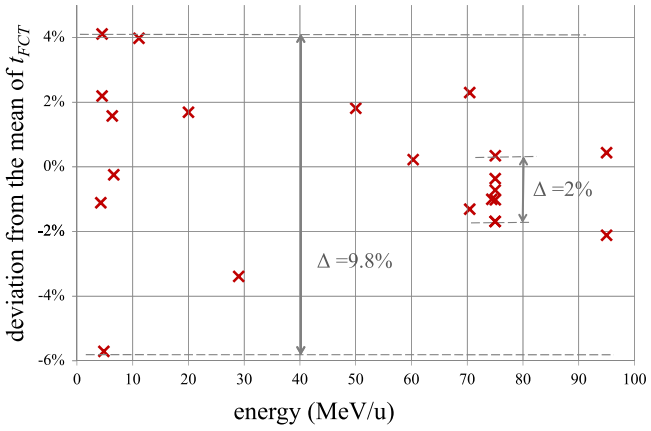

Fig. 11. Deviation from the mean of FCT transmittance versus energy.

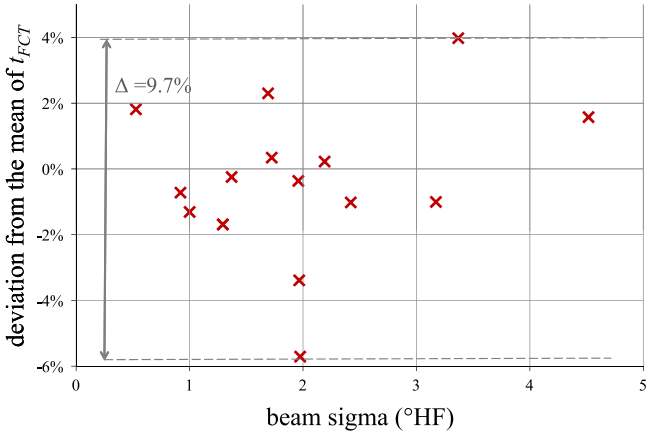

Fig. 12. Deviation from the mean of FCT transmittance versus beam sigma.

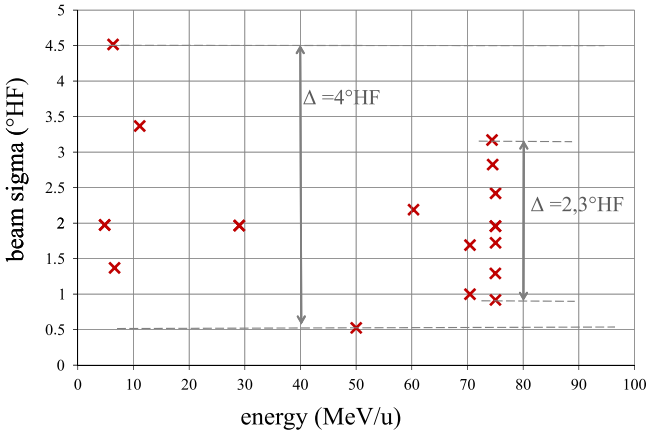

Fig. 13. Beam sigma versus energy.

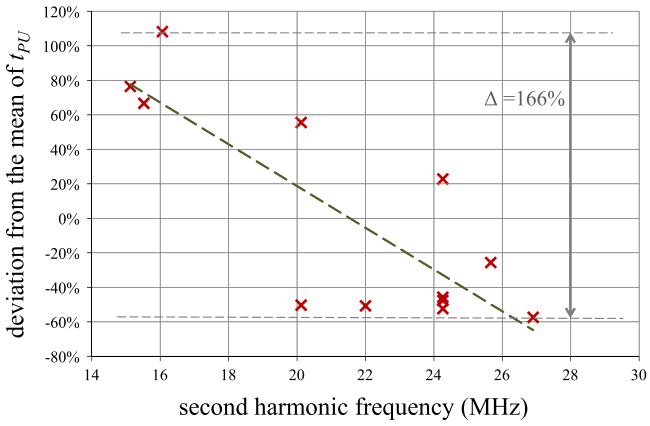

Fig. 14. Deviation from the mean of the PU transmittance versus second harmonic frequency.

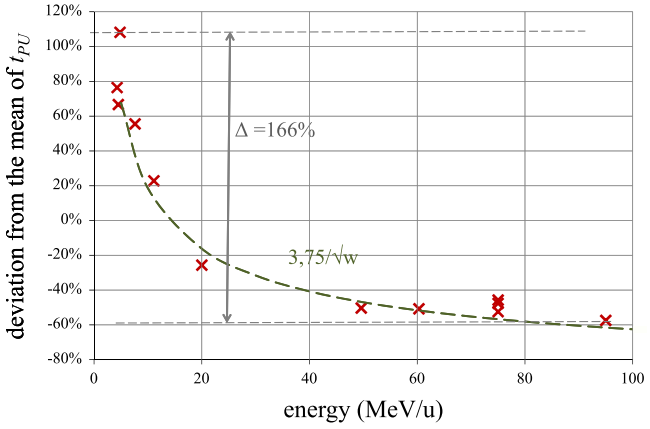

Fig. 15. Deviation from the mean of the PU transmittance versus energy.

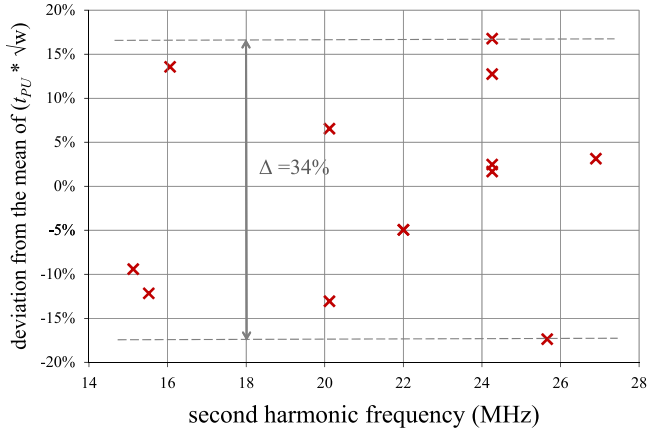

Fig. 16. Deviation from the mean of the PU transmittance versus frequency after energy sensitivity correction.

is then reduced from 166% to 34%. Moreover no sensitivity to pulse width is noted in Fig. 17.

The theoretical formula (3) with the dependence on the square root of energy is demonstrated. When the sensitivity to energy is taken into account, the uncertainty of measurement of the PU chain is reduced from ±83% to ±17%. This value remains broadly higher than the uncertainty measurement value of the FCT chain.

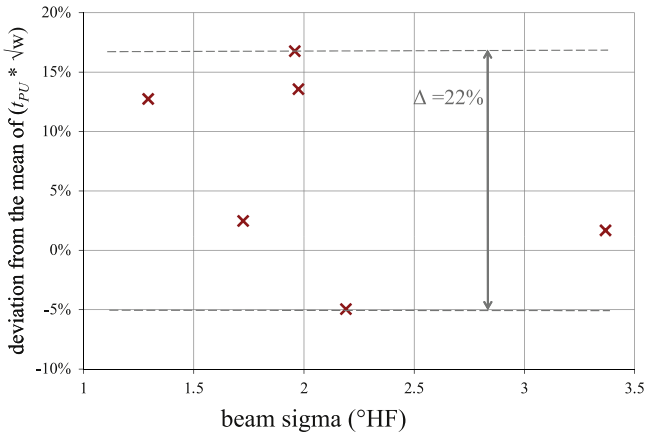

Fig. 17. Deviation from the mean of the PU transmittance versus beam sigma after energy sensitivity correction.

Table 2
Machine studies results.

Ion beam	F (MHz)	E (MeV/u)	Intensity range (nA)	σ_{beam} (° HF)	Deviation from the mean	
					FCT (%)	PU (%)
$^{12}_{6}C^{6+}$	94.98	13.45	0.9–1380		0.44	−57.4
$^{12}_{6}C^{6+}$	94.98	13.45	2–1850		−2.12	
$^{12}_{6}C^{6+}$	75.04	12.13	1.5–2500	2.42	−1.02	
$^{13}_{6}C^{6+}$	75.04	12.13	4.5–2500	1.72	0.34	−52.4
$^{12}_{6}C^{6+}$	75.01	12.13	0–2500	0.92	−0.72	
$^{12}_{6}C^{6+}$	75.00	12.13	0.8–1410	1.29	−1.69	−47.6
$^{13}_{6}C^{5+}$	11.11	12.13	1–3000	3.37	3.98	22.8
$^{12}_{6}C^{2+}$	6.60	9.38	1.5–1500	1.37	−0.24	
$^{14}_{7}N^{5+}$	20.00	12.83	1–120		1.69	−25.6
$^{18}_{8}O^{8+}$	75.01	12.13	17–2000	1.96	−0.36	−45.7
$^{18}_{8}O^{8+}$	50.00	10.10	6.1–86	0.53	1.81	
$^{40}_{20}Ca^{7+}$	4.50	7.76	2.4–720		2.19	66.7
$^{40}_{20}Ca^{8+}$	4.50	7.76	13–54		4.11	
$^{50}_{22}Ti^{10+}$	4.82	8.03	2–3500	1.98	−5.71	108.2
$^{58}_{28}Ni^{26+}$	74.40	12.10	800–1640	3.17	−1.00	
$^{78}_{36}Kr^{33+}$	70.44	11.80	15–1500		2.30	
$^{78}_{36}Kr^{33+}$	70.44	11.80	0–600	1.00	−1.31	
$^{86}_{36}Kr^{34+}$	60.30	11.00	2–2100	2.19	0.22	−50.7
$^{82}_{36}Kr^{11+}$	4.27	7.56	900-1300		−1.11	76.5
$^{208}_{82}Pb^{56+}$	29.00	7.82	19–100	1.97	−3.39	
$^{231}_{92}U^{31+}$	6.33	9.19	6–90	4.52	1.58	

7.6. Summary results

Table 2 summarizes the results achieved with FCT and PU and various beams from GANIL accelerators. The various beam intensity ranges are also described.

8. Conclusion

Due to the need of demonstrating the reliability of this safety system based on a beam diagnostic, a QA/QC Process is followed. A feasibility study has already been done. Simulations, tests in laboratory and machine studies have also been performed. Numerous tests have been done to characterize the sensitivity to energy, frequency and pulse width and to evaluate linearity and measurement uncertainty.

During machine studies a large panel of ion beams was tested and none was overlooked: for instance, a strongly chopped titanium beam

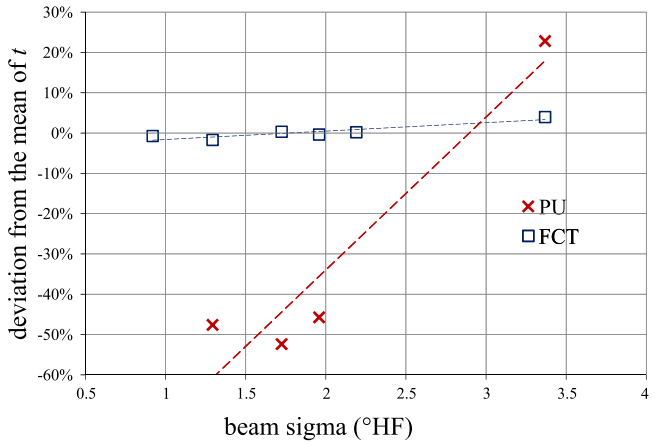

Fig. 18. Deviation from the mean of the PU/FCT transmittance versus beam sigma.

can be mentioned. Some of these cases should not be concerned by intensity monitoring. The worst case was estimated. Moreover no typical value has been calculated in the uncertainty calculation, which is thus maximized. Lastly, let us recall that part of the uncertainty is due to measurement chain modifications that may have occurred during these 2 years of machine studies.

As for PU, a strong sensitivity to the square root of energy has been demonstrated. Measurements are thus in good agreement with the theory. When this dependence is taken into account the uncertainty of measurement is reduced from $\pm 83\%$ to $\pm 17\%$. Concerning the FCT, no sensitivity is observed and its uncertainty of measurement is $\pm 4.9\%$ whatever influence quantities are considered.

The phase extension sensitivity has not been observed in machine studies due to the interference generated by some other quantities. When only machine studies done within short period of time with the same frequency and same ion are taken into account, the beam sigma sensitivity is clearly observed. Fig. 18 shows that the enlargement of the signal due to electric field is 15 times superior to the enlargement due to magnetic field. Let us recall that simulation results suggested a factor of ten.

As for linearity, the FCT offers a better linearity than PU. The linearity deviation of FCT is 5% at 10 nA and not 5 nA as expected. Due to the loss of precision of the reference measurement, these results may be assumed to be better.

In regards to uncertainty values, beam sigma sensitivity and linearity, only FCT can meet our specifications. The FCT, developed by Bergoz Instrumentation, associated to the SR844 constitutes a reliable system. This system is robust and shows little sensitivity to frequency, energy and bunch length.

Acknowledgments

This research was supported by GANIL and the head of the safety re-examination of existing GANIL facilities, Bertrand Rannou. Many colleagues contributed to these measurements and investigations, in particular, Christophe Jamet, William Le Coz and Ghislain Ledu. The authors are grateful to Joël James and Philippe Gaté for their technical assistance during installation of diagnostics and would like to thank John Frankland, Julien Bergoz, Frank Stulle and Guillaume Normand for comments that greatly improved the paper. The excellent support from the numerous teams involved in preparing and running GANIL is also acknowledged. Finally we are grateful to the Bergoz team for its efforts to develop the FCT.

References

[1] B. Jacquot, et al., Ganil status report, in: 17th International Conference on Cyclotrons and their Applications, Tokyo, 2004.
[2] E. Baron, Le grand accélérateur national d'ions lourds (GANIL), in: 5th Fast Ion Spectroscopy International Conference on Beam-Foil Spectroscopy, Journal of Physics Colloques, 40 (1979).
[3] C. Jamet, et al., THI safety system, in: Proceedings of DIPAC, France, 2005.
[4] P. Forck, Lectures Notes on Beam Instrumentation and Diagnostics, Juas, 2012.
[5] ⟨http://www.bergoz.com⟩.
[6] C. Nantista, C. Adolphsen, Beam current monitors in the NLCTA, in: Proceedings of the 1997 Particle Accelerator Conference (IEEE, New York, 1998) pp. 2186–2188 (SLAC-PUB-7523).
[7] P. Strehl, Beam Instrumentation and Diagnostics, Springer Verlag, ISBN-10 3-540-26401-9, p. 161, Berlin, 2006.
[8] M. Cohen-Solal, Physical Review of Selected Topics on Accelerators and Beams 13 (2010).
[9] C.K. Allen, N. Brown, M. Reiser, Particle Accelerators 45 (1994) 149.
[10] J.R. Harris, Longitudinal effects and focusing in space charge (thesis), University of Maryland, 2002.
[11] A. Hofmann, Dynamics of beam diagnostics, CERN Accelerator School, Geneva, Switzerland, 2009.
[12] F. Caspers, Handbook of Accelerator Physics and Engineering, 2nd edition, Bench measurements, 2013, p. 745.
[13] J.D. Jackson, Classical Electrodynamics, John Wiley & Sons Inc., New York, 1975.
[14] M. Reiser, Theory and Design of Charged Particle Beams, John Wiley & Sons, New York, 2008.
[15] J.C. Denard, Beam Current Monitors, CERN Accelerator School on Beam Diagnostics, Dourdan, France, 2008.